

# Morphology and porous texture of iron fine particles with relation to their magnetic properties

T. SUEYOSHI

*Hitachi Maxell Ltd, Oyamazaki Otokuni, Kyoto 618, Japan*

The effects of silica film as thin as 0.4 nm on the variation of morphology of particles, in the process of reduction of microporous haematite particles with hydrogen gas, were investigated by means of gas adsorption, electron microscopy, X-ray diffraction and magnetic measurements. Microporous haematite particles were prepared by decomposition of the silica-coated goethite particles. A silica film of 0.4 nm thickness was coated on the surface of the goethite particles (length: 400 nm, width 25 nm). In the process of reduction, collapse and sintering of the particles were markedly suppressed by coating with ultra-thin silica film. In the reduced particles, iron crystallites were separated from each other forming iron particles of large porosity. By introducing heat-treatment of the silica-coated haematite particles at 700°C in air prior to reduction, highly acicular iron particles having the crystallites grown along the elongated direction of the particles were obtained. A marked increase in the coercivity of the iron particles from 1075 to 1530 Oe was attributed to the increase of the shape anisotropy.

## 1. Introduction

Studies on high density recording media such as magnetic audio and video tapes, floppy discs and so on have been more and more active along with a remarkable development of the recording technology. For the purpose of getting high density recording media having high frequency response and high signal to noise ratio, magnetic fine particles for the particulate recording media, such as  $\gamma\text{-Fe}_2\text{O}_3$  particles, cobalt-modified  $\gamma\text{-Fe}_2\text{O}_3$  particles, and metal particles, have been improved not only by increasing their coercivity and magnetization but also by decreasing their size while keeping their narrow size distribution. As for the iron-based metal particles, there have been a number of studies with respect to the preparation and to their magnetic properties because of their excellent magnetic properties and applicability in practical use [1-3].

Preparation methods of the iron-based metal particles so far proposed are divided into the following four main methods. They are (i) electrodeposition into mercury [4, 5], (ii) the reduction of ferrous salt in aqueous solution with  $\text{NaBH}_4$  [6], (iii) deposition from the vapour phase [7], and (iv) the thermal decomposition and following reduction of oxalates, oxides and oxyhydrates in hydrogen gas [8]. In order to get highly acicular iron fine particles having high coercivity and large magnetization, suitable for getting magnetic media with high recording density, we have been examining the method that makes use of the reduction of haematite particles prepared from acicular goethite particles. It is well known that the magnetic properties of iron particles have a close relation to particle size, acicularity and porosity. Therefore, to determine the optimum preparation condition of iron particles, it is

important to make clear the relationship between their morphology and magnetic properties.

In our previous report [9], we were able to pursue the characteristic variation in morphology of microporous haematite particles during their reduction process. In addition, we also described the strong suppression effect against the sintering and collapse of the iron particles by silica coating and alumina coating. It was also found that the coercivity of iron particles was markedly dependent on their crystallite size, and that the crystallite size was controlled by introducing both surface treatment on goethite particles and following heat-treatment prior to reduction in hydrogen gas [10, 11].

In this report, the effects of ultra-thin silica film, coated on the surface of the particles, on the variation in morphology and magnetic properties of the particles will be discussed from the standpoint of the microscopic observation of the particles by the adsorption technique, electron microscopy, X-ray diffraction and magnetic measurements.

## 2. Experimental procedure

Acicular goethite particles (length: 400 nm, width: 20 nm) were synthesized by the oxidation of ferrous hydroxide gel in an aqueous NaOH solution, prepared by mixing 100 ml of 0.7 M ferrous sulphate solution with 100 ml of 4 N NaOH solution. The shape and size of the goethite particles were determined by controlling reaction conditions such as reaction temperature, stirring speed, amount of air introduced into the reaction mixture for oxidation, and NaOH concentration. Silica film was coated on the surface of the goethite particles by the following method. In 2 litres of 0.5 N NaOH solution, 20 g of goethite particles were

dispersed, and 20 ml of 1 M aqueous  $\text{Na}_4\text{SiO}_4$  solution was poured into the suspension. Then,  $\text{CO}_2$  gas was introduced into this suspension in order to neutralize the alkaline solution until the pH value decreased and reached less than 9. The dispersion was washed with distilled water until the supernatant liquid indicated a constant electrical conductivity. Finally, the suspension was filtered and dried at  $60^\circ\text{C}$  to get the silica-coated ( $\text{Si}/\text{Fe} = 2 \text{ wt}\%$ ) goethite particles.

Haematite particles with slit-shaped micropores, the starting material for reduction, were prepared by decomposition of the silica-coated goethite particles at  $250^\circ\text{C}$  *in vacuo*. The reaction apparatus for decomposition and reduction of the particles was the same as that used in previous experiments [9], and the degree of decomposition and reduction were determined by measuring the amount of water trapped with a cold trap. Nitrogen gas adsorption isotherms were measured by a volumetric adsorption apparatus which was directly connected to the reaction apparatus. Powder X-ray diffraction patterns were measured by an X-ray diffractometer (Rigakudenki Geigerflex SG-7) using an iron target and manganese filter under the conditions of 40 kV and 20 mA. The morphology of the particles was observed by transmission electron microscopy (Hitachi H-700H). The magnetic properties of the reduced samples were measured by a vibrating sample magnetometer (Toeikogyo VSM-3) under a maximum applied field of 10 kOe.

### 3. Results and discussion

#### 3.1. Decomposition of silica-coated goethite particles

Silica-coated goethite particles were decomposed to form haematite particles by the following dehydration

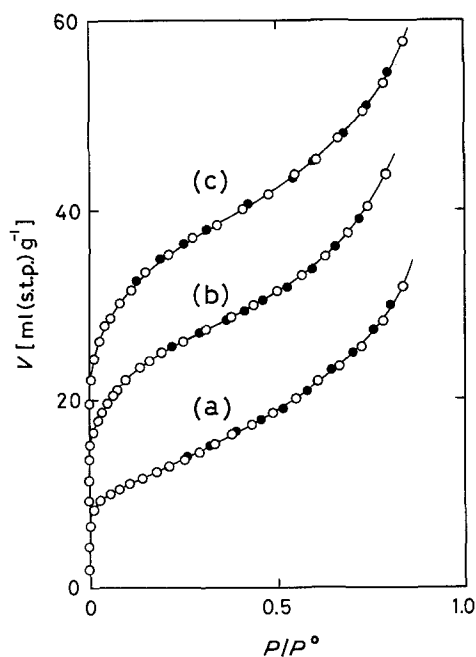


Figure 1 Adsorption isotherms of  $\text{N}_2$  gas on to silica-coated particles at 77 K. (○) Adsorption, (●) desorption. (a) Silica-coated goethite particles pretreated at  $25^\circ\text{C}$  for 8 h *in vacuo*.  $S_{\text{BET}}: 46 \text{ m}^2 \text{ g}^{-1}$ . (b) 79% decomposed particles pretreated at  $200^\circ\text{C}$  for 6 h *in vacuo*.  $S_{\text{BET}}: 87 \text{ m}^2 \text{ g}^{-1}$ . (c) 100% decomposed microporous haematite particles pretreated at  $250^\circ\text{C}$  for 2 h *in vacuo*.  $S_{\text{BET}}: 125 \text{ m}^2 \text{ g}^{-1}$ .

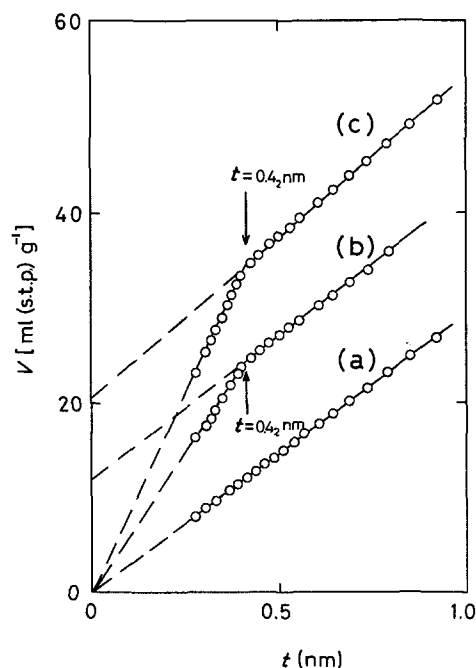
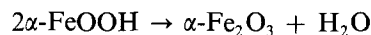


Figure 2 de Boer's  $t$  plot.

reaction at a temperature above ca.  $150^\circ\text{C}$ :



Nitrogen gas adsorption isotherms at 77 K on to the silica-coated goethite particles, their partially dehydrated particles, and the completely dehydrated microporous haematite particles prepared by decomposition at  $250^\circ\text{C}$  *in vacuo* are shown in Fig. 1. These isotherms for the decomposed particles are nearly parallel to that for the initial non-porous goethite particles. They shift to the higher adsorption volume region with progress in the degree of decomposition, reaching the highest adsorption volume for the sample decomposed at  $250^\circ\text{C}$  for 2 h *in vacuo*. In addition, they show no hysteresis loop in adsorption and desorption branches of the isotherms in the course of decomposition at the temperatures below ca.  $250^\circ\text{C}$ . These results suggest the formation of micropores by decomposition of the goethite particles. In order to clarify the texture of the haematite particles, de Boer's  $t$  plot was performed on these isotherms, taking the isotherm for the non-porous goethite particles as an internal standard for evaluation of the thickness ( $t$ ) of the adsorbed layer in the manner reported by Naono and Fujiwara [12]. As shown in Fig. 2, the sharp bending point in the  $t$  plot at  $t = 0.42 \text{ nm}$  indicates the formation of slit-shaped micropores of 0.8 to 0.9 nm width in all silica-coated haematite particles, which is almost the same as was previously observed in the case of the non-coated samples [9]. As shown in Fig. 3, an electron micrograph of the silica-coated haematite particles confirms the formation of slit-shaped micropores of ca. 1 nm width, opened along the elongated direction of the acicular haematite particles. It also indicates that the coated silica film on the surface of the particles hardly influenced the formation of the slit-shaped micropores, and that the skeleton of the precursor was maintained almost unchanged during formation of these slit-shaped micropores. In addition, it is found that the surface

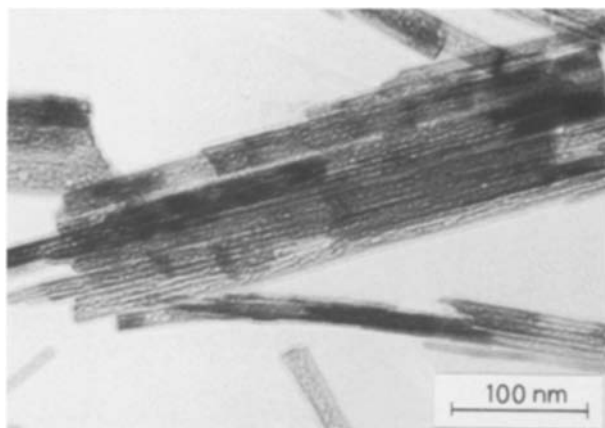


Figure 3 Electron micrograph of slit-shaped microporous haematite particles.

area of the particles was hardly influenced by the coated silica thin film, which suggests uniformity of the silica thin film on the surface of the particles.

### 3.2. Heat treatment of the microporous haematite particles

Microporous haematite particles, prepared by decomposition of the goethite particles at 250°C *in vacuo*, were heat-treated at various temperatures above 250°C in air. Nitrogen gas adsorption isotherms at 77 K for the silica-coated and for the non-coated haematite particles are shown in Figs 4 and 5, respectively. Adsorption isotherms shifted to the lower side as heat-treatment temperature increased above ca. 300°C because of the formation of mesopores by aggregation of the slit-shaped micropores, and the consequent decrease in surface area of the particles. Compared with the non-coated samples shown in Fig. 5, the isotherms for the silica-coated samples, as shown in Fig. 4, did not abruptly decrease in their

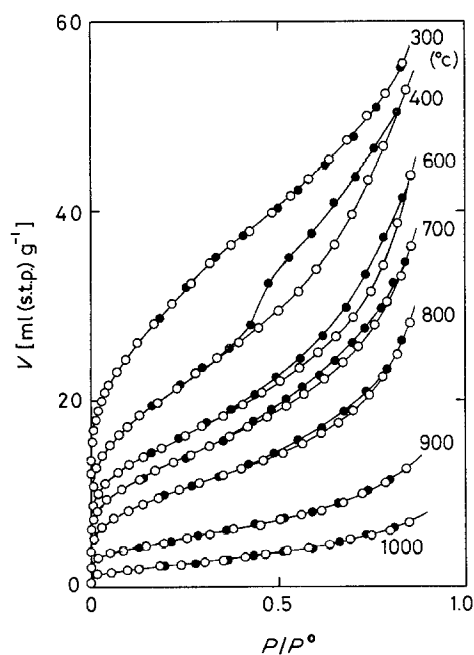


Figure 4 Adsorption isotherms of N<sub>2</sub> gas on to silica-coated haematite particles pretreated at various temperatures. (O) Adsorption, (●) desorption.

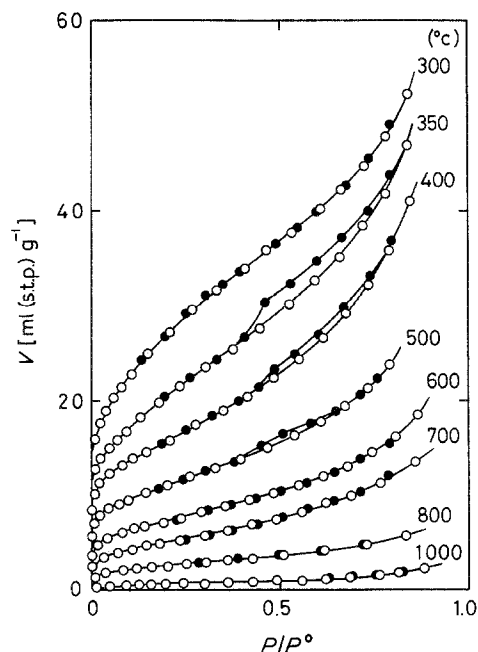


Figure 5 Adsorption isotherms of N<sub>2</sub> gas on to non-coated haematite particles pretreated at various temperatures. (O) Adsorption, (●) desorption.

adsorption volume of nitrogen with increase in heat-treatment temperature, which is considered to be due to the suppression of sintering of the particles by the coated silica thin film. Variations in specific surface area ( $S_{BET}$ ) of the haematite particles, derived from these isotherms using the BET equation, are shown in Fig. 6. The difference of  $S_{BET}$  between non-coated and silica-coated samples increased with increase in heat-treatment temperature, and reached a maximum at 700 to 800°C. As shown in Figs 7 and 8, an effect of the silica coating on the morphology of the haematite particles can be clearly observed. Granular haematite particles were obtained by heat-treatment of the non-coated sample at 700°C, whereas highly acicular

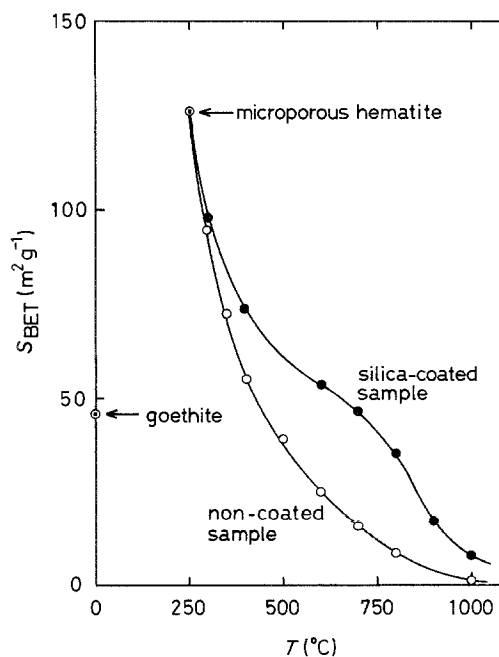


Figure 6 Variation in specific surface area ( $S_{BET}$ ) of haematite particles with heat-treatment temperature.

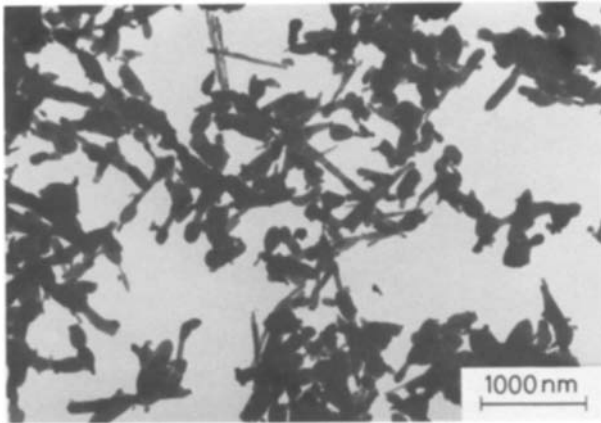
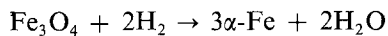
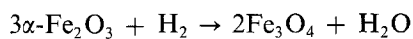


Figure 7 Electron micrograph of non-coated haematite particles treated at 700°C in air.

haematite particles with densely packed structure were prepared by heat-treatment of the silica-coated samples.

### 3.3. Reduction of the silica-coated haematite particles

The silica-coated microporous haematite particles were chosen as a starting material for reduction in hydrogen gas. Reduction proceeded by the following reactions:



Nitrogen gas adsorption isotherms for the particles, prepared by reduction of the silica-coated microporous haematite particles, are shown in Fig. 9. The appearance of the hysteresis loops of adsorption and desorption branches of these isotherms suggest that the shape of the pores significantly changed from the slip-shaped micropores to mesopores with progress of the degree of reduction. Based on these isotherms, pore volume and pore size distributions could be estimated by means of the method of Roberts [13]. As shown in Fig. 10, the pore size distribution clearly indicates that the pores changed from micropores (size: 2 nm) to mesopores (size: 2 to 50 nm) [14] as the degree of reduction was increased. However, the pore

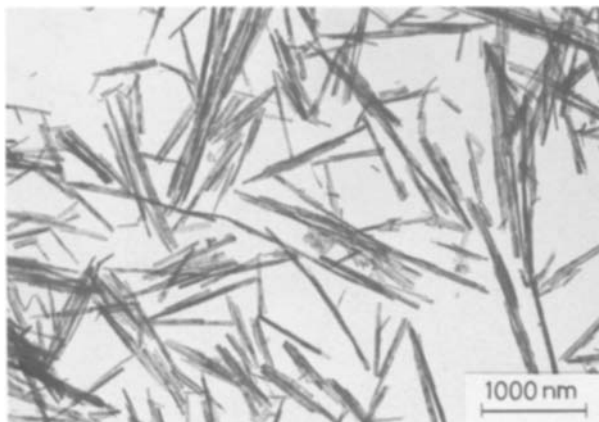


Figure 8 Electron micrograph of silica-coated haematite particles treated at 700°C in air.

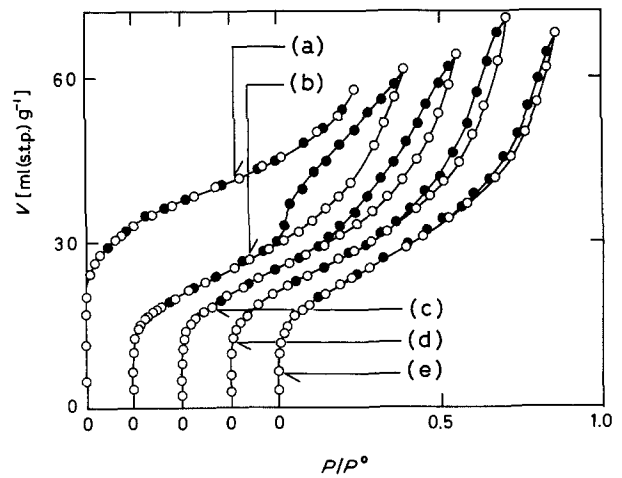


Figure 9 Adsorption isotherms of  $\text{N}_2$  gas on to silica-coated particles at 77 K. (○) Adsorption, (●) desorption. (a)  $R = 0\%$ ,  $S = 125 \text{ m}^2 \text{ g}^{-1}$ ,  $V_p = 0.047 \text{ ml g}^{-1}$ ; (b)  $R = 11$ ,  $S = 81$ ,  $V_p = 0.005$ ; (c)  $R = 43$ ,  $S = 48$ ,  $V_p = 0.008$ ; (d)  $R = 90$ ,  $S = 48$ ,  $V_p = 0.004$ ; (e)  $R = 100$ ,  $S = 42$ ,  $V_p = 0.001$ .

volume ( $V_p$ ) was maintained at a nearly constant value of  $0.05 \text{ cm}^3 \text{ g}^{-1}$  during the reduction process. Calculated from the  $V_p$  for the silica-coated iron particles of  $R = 97\%$ , their porosity was found to be more than 30%. It means that highly porous particles were prepared by reduction of the silica-coated microporous haematite particles.

The arrangement of the iron crystallites and pores in each particle was observed in detail by transmission electron microscopy. Electron micrographs of the reduced samples are shown in Fig. 11. It was clearly observed that the acicularity of the precursor was kept unchanged during reduction of the haematite particles due to the suppression effect of the silica film against collapse and sintering of the particles. However, owing to the decrease of the net volume of the particles along with growth of iron crystals, the iron crystallites formed in each particle were separated from each other by the pores, and they increased in size as the degree of reduction was increased. Although silica

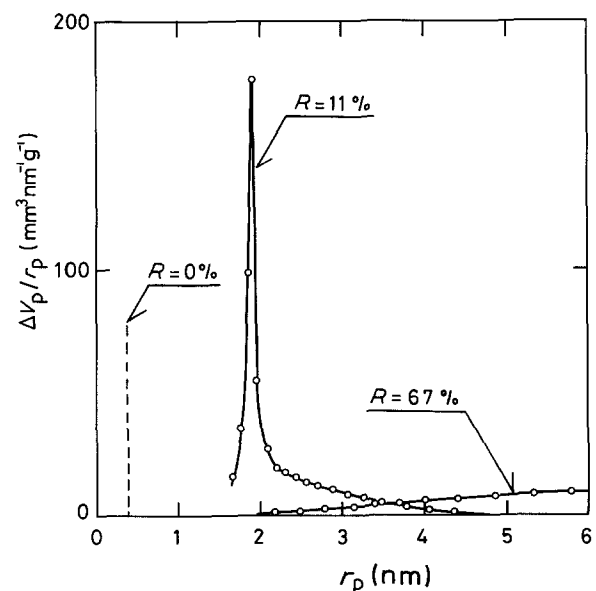


Figure 10 Pore size distributions of silica-coated particles.

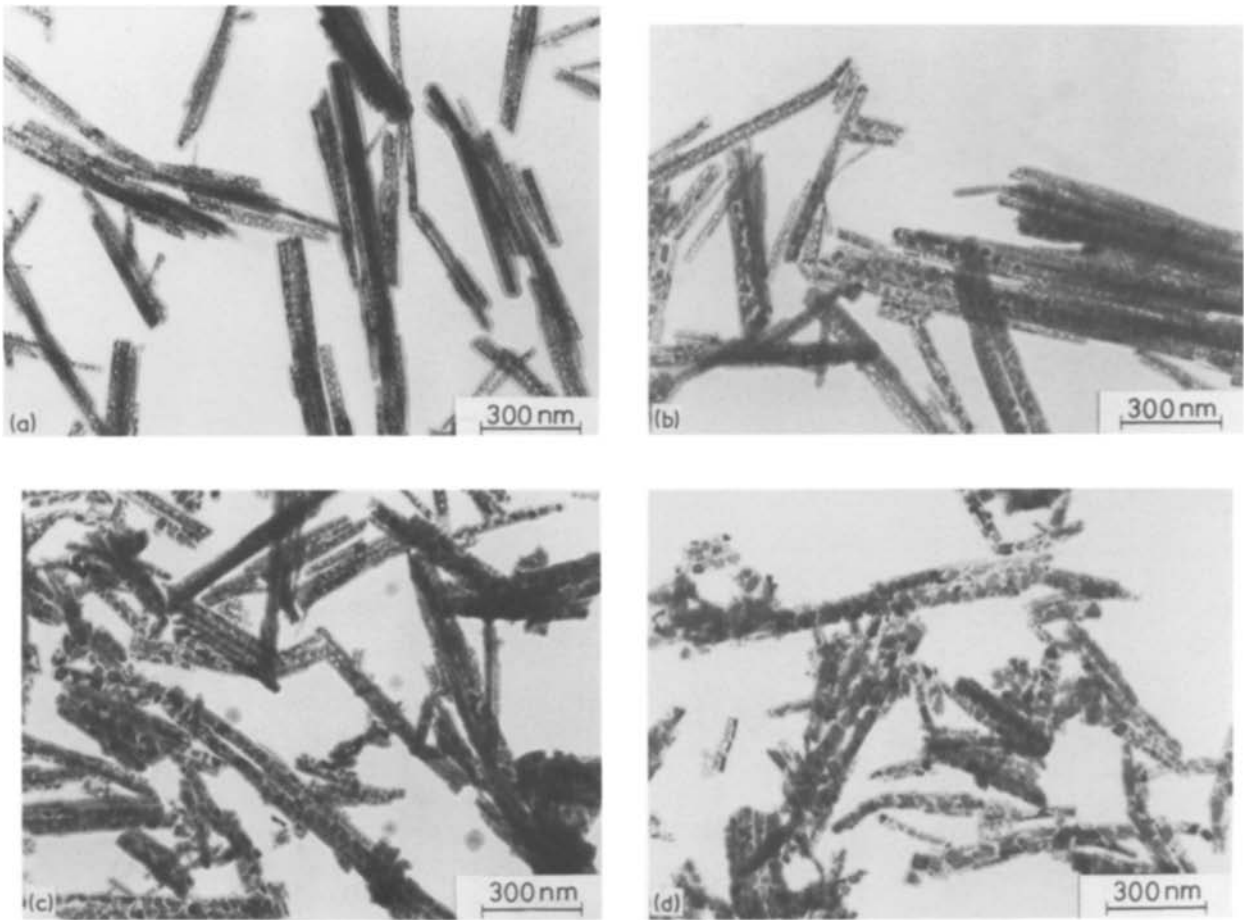


Figure 11 Electron micrographs of reduced particles: (a)  $R = 11\%$ , (b)  $R = 29\%$ , (c)  $R = 67\%$ , (d)  $R = 97\%$ .

coating has the advantage of preventing the reduced particles from sintering and collapse, it also has the disadvantage of increasing the porosity of the particles.

X-ray diffraction patterns for the haematite particles and their reduced particles are shown in Fig. 12. The diffraction patterns indicate the change from haematite to magnetite in the range of  $0 \leq R \leq 10\%$ , followed by the change from magnetite to iron in the range of  $10 \leq R \leq 100\%$ . No diffraction peak of FeO crystals was observed in our experimental condition, which is consistent with the results reported by Klissurski *et al.* [15]. As shown in the upper part of Fig. 12, the diffraction pattern of the silica-coated samples is just the same as that of the non-coated samples except that the width of the X-ray diffraction line broadening indicates a difference in the crystallite size of the iron particles. By making a silica coating on the surface of the particles, crystal growth of the iron crystallite was found to be fairly suppressed.

In order to increase the acicularity and decrease the porosity of the silica-coated iron, the silica-coated haematite particles which were treated at  $700^\circ\text{C}$  in air prior to reduction were reduced in hydrogen gas. By heat-treatment of the silica-coated haematite particles,  $S_{\text{BET}}$  and  $V_p$  of the particles significantly decreased from  $125$  to  $47\text{ m}^2\text{ g}^{-1}$  and from  $0.047$  to less than  $0.001\text{ cm}^3\text{ g}^{-1}$ , respectively, while keeping their original high acicularity. Consequently, highly acicular haematite particles of densely packed structure were obtained by introducing the heat-treatment at high

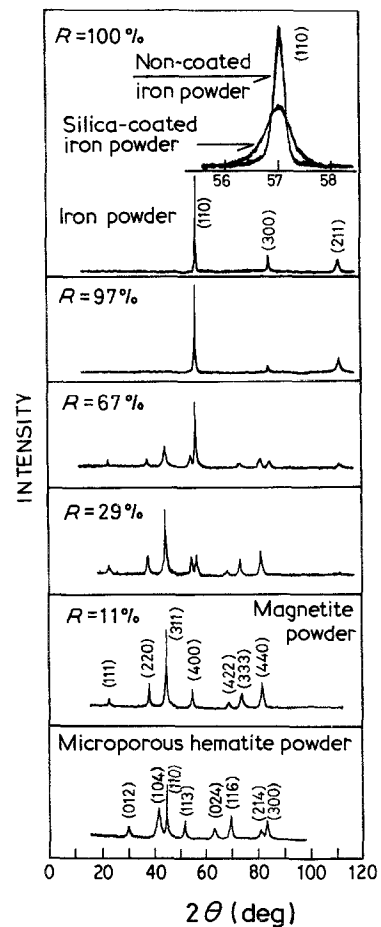


Figure 12 Powder X-ray diffraction patterns.

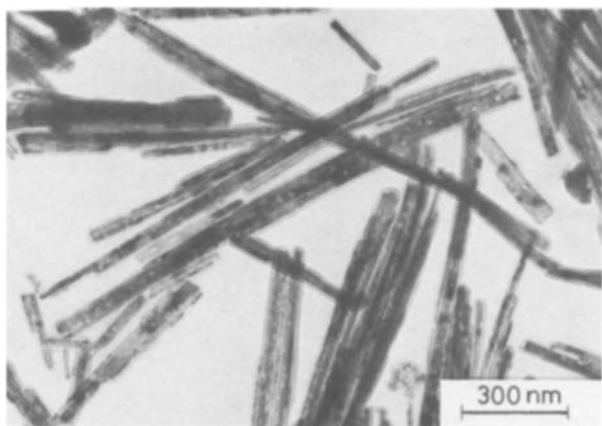


Figure 13 Electron micrograph of silica-coated haematite particles treated at 700°C in air.

temperatures. As shown in Fig. 13, electron micrographs of the haematite particles treated at 700°C clearly demonstrates the effect of the silica coating described above.

Nitrogen gas adsorption isotherms at 77 K on to the silica-coated haematite particles treated at 700°C in air, and on to their reduced samples in hydrogen gas, are shown in Fig. 14. On closer investigation of these isotherms, it was realized that nearly non-porous iron particles having extremely low porosity were prepared at  $R = 90$  to 100%, even though the pore volume slightly increased at the initial stage of reduction owing to a deoxidation reaction. The pore volume of these particles was extremely small over the whole range of reduction degree, in comparison with that of the samples previously described in Fig. 9. The electron micrograph of the iron particles shown in Fig. 15a confirmed the formation of highly acicular iron fine particles of low porosity by introducing heat-treatment to the silica-coated haematite particles prior to reduction at 500°C in hydrogen gas. On the other hand, as shown in Fig. 15b, granular iron particles were obtained by reduction of the non-coated microporous haematite particles at 500°C in hydrogen gas.

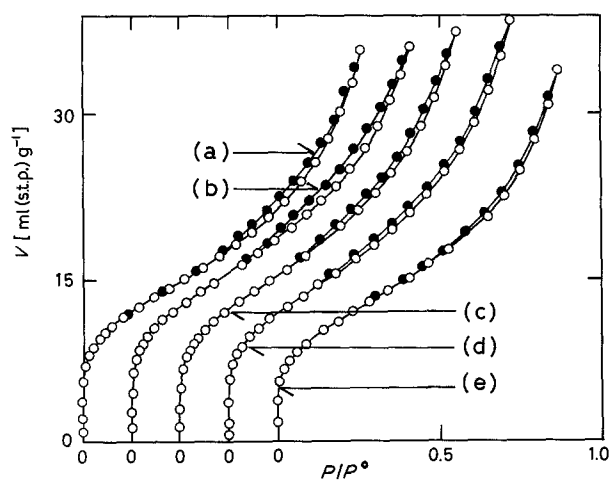


Figure 14 Adsorption isotherms of  $N_2$  gas on to silica-coated and heat-treated particles at 77 K. (O) Adsorption, (●) desorption. (a)  $R = 0\%$ ,  $S = 47 \text{ m}^2 \text{ g}^{-1}$ ,  $V_p = 0.001 \text{ ml g}^{-1}$ ; (b)  $R = 18$ ,  $S = 49$ ,  $V_p = 0.005$ ; (c)  $R = 43$ ,  $S = 48$ ,  $V_p = 0.008$ ; (d)  $R = 90$ ,  $S = 48$ ,  $V_p = 0.004$ ; (e)  $R = 100$ ,  $S = 42$ ,  $V_p = 0.001$ .

As for the coated silica film which influenced markedly the morphology and magnetic properties of the iron particles, it is considered that it consists of a fairly thin film which uniformly covers the surface of the particles because of the following reasons. Firstly, collapse and sintering of the silica-coated particles, which were unavoidable for the non-coated particles, can be completely suppressed even in the case of heat-treated samples at elevated temperatures above 700°C. Secondly, there is no appreciable increase of  $S_{\text{BET}}$  of the particles along with silica-coating: i.e., the coated silica hardly contributes to the  $S_{\text{BET}}$  of the particles. The increase in  $S_{\text{BET}}$  can be expected to be at least  $5 \text{ m}^2 \text{ g}^{-1}$  by silica coating at  $\text{Si/Fe} = 2 \text{ wt } \%$ , provided the coated silica exists heterogeneously on the surface of the particles. From the results described above, it can be estimated that the silica film consists of an ultra-thin film of nearly monomolecular thickness of ca. 0.4 nm, and it adopts a planar network structure through which molecules such as hydrogen, nitrogen and water vapour can easily permeate.

It is well known that the coercivity of the magnetic particles is mainly dependent on (i) magnetocrystalline anisotropy, (ii) shape anisotropy and (iii) magnetostrain anisotropy. As to the iron particles, Kittel [16] calculated from theoretical considerations that the contribution of each magnetic anisotropy to the coercivity is (i) 500 Oe, (ii) 10700 Oe and (iii) 600 Oe, respectively. His result suggests that the shape anisotropy plays a determining role in the coercivity of iron particles. Accordingly, the magnetic properties of acicular iron particles must have a close relation to their morphology. Suzuki and co-workers [17–19] reported a correlation between coercivity and macropore size of iron particles determined by the mercury penetration method, and suggested the formation of a stereo-network structure for the iron particles prepared by decomposition and following reduction of iron oxalate and iron oxyhydrate.

In order to investigate the relationship between morphology and magnetic properties of the ultra-fine particles in detail, it is considered to be reasonable to examine small pores such as micropores and mesopores by means of the gas adsorption technique. According to the experimental results we reported previously [10], a silica thin film coated on the surface of the iron particles significantly influenced their morphology. As shown in our previous paper [9], non-coated iron particles easily increased their size in the process of reduction, resulting in a sintering among particles and the collapse of their original acicular

TABLE I Magnetic properties, crystallite size and specific surface area of iron particles\*

Sample	$H_c$ (Oe)	$M_s$ (e.m.u. $\text{g}^{-1}$ )	$M_r/M_s$	C.S. (nm)	$S_{\text{BET}}$ ( $\text{m}^2 \text{ g}^{-1}$ )
A	375	190	0.23	~90	9
B	1075	135	0.46	20.5	82
C	1530	155	0.54	21	42

\* Sample A: non-coated, Sample B: silica-coated ( $\text{Si/Fe} = 2 \text{ wt } \%$ ), Sample C: silica-coated and heat-treated;  $H_c$ : coercivity,  $M_s$ : saturation magnetization,  $M_r/M_s$ : squareness, C.S.: crystallite size,  $S_{\text{BET}}$ : specific surface area.

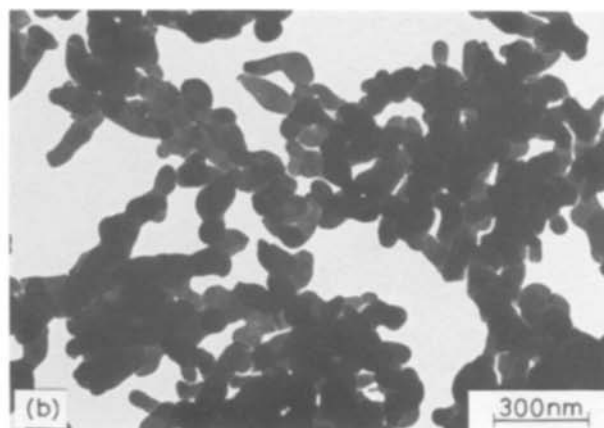
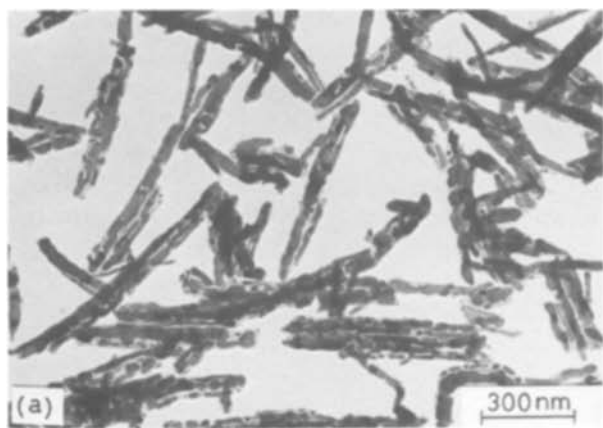


Figure 15 (a, b) Electron micrographs of iron particles.

shape. Consequently, their coercivity markedly decreased their shape anisotropy decreased and their crystallite size increased to a value larger than the crystal size of single-domain behaviour.

The magnetic properties and crystallite size of iron particles are shown in Table I. It is obvious that the coercivity of silica-coated iron particles (Sample B), prepared by reduction at 500°C for 2 h in hydrogen gas, is more than 2 times as large as that of the non-coated iron particles (Sample A). The coercivity of iron particles further increased by introducing heat-treatment at 700°C to the silica-coated haematite particles prior to reduction, and reached 1530 Oe while keeping their original acicular shape and their crystallite size of ca. 21 nm. Such a drastic increase in coercivity by more than 30% is mainly attributed to the increase of shape anisotropy of iron particles. Electron diffraction patterns of the heat-treated sample (Sample C), which has a highly acicular shape and low porosity, showed the clear diffraction pattern of iron single-like crystals; whereas Sample B, the directly reduced iron particles, showed no clear diffraction pattern. Therefore, it is considered that Sample C, which was subjected to heat treatment at the temperature of 700°C, crystallized well along the elongated direction of the particles producing a large shape anisotropy.

#### 4. Conclusions

1. In the process of reduction of haematite particles, collapse and sintering of the particles were suppressed by coating with an ultra-thin silica film of 0.4 nm thickness.

2. Iron crystallites in an iron particle were separated from each other by direct reduction of the silica-coated microporous haematite particles to form highly porous iron particles having a porosity of ca. 30%.

3. By introducing heat-treatment to the silica-coated haematite particles at 700°C in air prior to reduction, highly acicular iron particles were obtained.

4. A marked increase in coercivity of the iron particles up to 1530 Oe was mainly attributed to an increase of the shape anisotropy.

#### Acknowledgements

The author is grateful to Professor Hiromitsu Naono

of Kwansai Gakuin University for his invaluable discussions and suggestions throughout this work. He is also grateful to Drs Masahiro Amemiya, Fumitada Hayama and Mikio Kishimoto for technical discussions and encouragement.

#### References

1. M. KAWASAKI and S. HIGUCHI, *IEEE Trans. Magn.* **MAG-8** (1972) 430.
2. A. A. Van der GIESSEN, *ibid.* **MAG-9** (1973) 191.
3. A. H. MORRISH and P. J. PICONE, in *Ferrites: Proceedings of International Conference of Ferrites, Kyoto*. Edited by H. Watanabe, S. Iida and M. Sugimoto (Center for Academic Publications, Japan, 1980) p. 613.
4. F. E. LUBORSKY and T. O. PAINE, *J. Appl. Phys.* **31** Suppl. (1960) 68S.
5. F. E. LUBORSKY, *ibid.* **32** Suppl. (1961) 171S.
6. A. L. OPPEGARD, F. J. DARNELL and H. C. MILLER, *ibid.* **32** Suppl. (1961) 184S.
7. K. KIMOTO, Y. KAMIYA, M. NONOYAMA and R. UEDA, *Jpn J. Appl. Phys.* **2** (1963) 702.
8. A. A. Van der GIESSEN and C. J. KLOMP, *IEEE Trans. Magn.* **MAG-5** (1969) 317.
9. T. SUEYOSHI, H. NAONO, M. KAWANAMI, M. AMEMIYA and F. HAYAMA, *ibid.* **MAG-20** (1984) 42.
10. T. SUEYOSHI, K. TASHITA, S. HIRAI, M. KISHIMOTO, Y. HAYASHI and M. AMEMIYA, *J. Appl. Phys.* **53** (1982) 2570.
11. T. SUEYOSHI, K. TASHITA, S. HIRAI, Y. HAYASHI and M. AMEMIYA, *J. Magn. Magn. Mater.* **31-34** (1983) 939.
12. H. NAONO and R. FUJIWARA, *J. Colloid Interface Sci.* **73** (1980) 406.
13. B. F. ROBERTS, *ibid.* **23** (1967) 266.
14. S. J. GREGG and K. S. W. SING, "Adsorption, Surface Area and Porosity", 2nd Edn (Academic Press, London, 1982) p. 25.
15. D. G. KLISSURSKI, I. G. MITOV and T. TOMOV, *Can. J. Chem.* **58** (1980) 1473.
16. C. KITTELL, *Rev. Mod. Phys.* **21** (1949) 541.
17. S. SUZUKI, Y. OMOTE, S. MIYA, I. YOSHIDA, A. ISHIDA, J. MINEGISHI and O. IWATARE, in *Ferrites: Proceedings of International Conference of Ferrites, Kyoto*. Edited by H. Watanabe, S. Iida and M. Sugimoto (Center for Academic Publications, Japan, 1980) p. 556.
18. S. SUZUKI, H. SAKUMOTO and Y. OMOTE, *J. Magn. Magn. Mater.* **31-34** (1983) 941.
19. S. SUZUKI, H. SAKUMOTO, J. MINEGISHI and Y. OMOTE, *IEEE Trans. Magn.* **MAG-17** (1981) 3017.

Received 4 April

and accepted 30 June 1986